

Computer Simulation of a FIR Filter for the MMA

R. Escoffier, L. R. D'Addario, C. Broadwell, J. Webber and F. Schwab
National Radio Astronomy Observatory

February 4, 1999

1. Introduction

MMA Memo 204 described a practical digital filter to be used in place of analog filters in the IF electronics of the MMA. This memo presents the results of computer simulations of the proposed digital FIR (finite impulse response) filter.

The main thrust of the simulations presented here was to demonstrate that digital filtering, with acceptable performance, could be performed using as the filter input the low amplitude resolution outputs of the 4-GHz sampler to be used in the MMA. Other important parameters to be determined before the actual FIR filter can be designed, such as the number of tap multiplications required and the arithmetic precision needed in the filter, were not specifically considered.

2. Simulation Software

Figure 1 shows the logical flow of the C language FIR simulation program used to generate frequency response plots presented in this memo.

The RANDOM NUMBER GENERATOR and CONVERT TO GAUSSIAN DISTRIBUTION blocks seen in Figure 1 were used to simulate the broadband output of an antenna receiver. Up to four independent sinusoids were added to this flat spectrum signal before sampling. The input sampler of Figure 1 (in the MMA, this would be the sampler module) could be selected to simulate either a 4-level or an 8-level quantizer.

The second stage sampler seen in Figure 1 is the stage at which the high precision computed FIR output was modified to match the 4-level configuration to be expected of the MMA correlator chip.

A 257-point lag autocorrelator was used for spectrum analysis. The 257-point value was chosen so that when lag channels were reflected over to lead channels, a full 512 point FFT could be done (with 255 lag channels, a zero lag channel, and 256 lead channels).

Quantization correction was done to correct for the 4-level sampler following the filter. No correction was done to correct for the sampler at the filter input. The quantization correction applied to the autocorrelator output in the simulation was that for a 4-level sampler with a driving signal having a Gaussian amplitude distribution. In actual fact, the signal driving to the output sampler was not Gaussian because of the action of the input sampler. Some preliminary work was done on the proper quantization correction that must be applied in the MMA using a digital filter, but more study needs to be done.

The sampler thresholds and sampler output weights used in the simulation program were selected for maximum correlator efficiency for both 4- and 8-level samplers (per Fred Schwab). Actual thresholds and weights are seen below:

4-level sampler:	T0 = - 0.98159883*rms	W0 = - 3.335875
	T1 = 0.0	W1 = - 1.0
	T2 = 0.98159883*rms	W2 = 1.0
		W3 = 3.335875
8-level sampler:	T0 = - 1.75*rms	W0 = - 8.78
	T1 = - 1.05*rms	W1 = - 5.48
	T2 = - 0.5*rms	W2 = - 3.08
	T3 = 0.0	W3 = - 1.00
	T4 = 0.5*rms	W4 = 1.00
	T5 = 1.05*rms	W5 = 3.08
	T6 = 1.75*rms	W6 = 5.48
		W7 = 8.78

3. Filters Simulated

A digital filter suitable for use in the MMA would be programmable to allow array operations with bandwidths from 2 GHz to 31.25 MHz (or lower) per BB channel. This programmability would have the form of selectable tap weights and a versatile structure to trade off the number of tap weights for bandwidth. If, for example, a filter with 128 tap weights were designed for 1 GHz bandwidth operation, the same logic could be configured to provide 256 tap weight multiplications with 500 MHz observations. In general, the number of tap weight multiplications available will go in binary steps from 128 to 4096 as the output bandwidth goes from 2 GHz to 31.25 MHz (for bandwidths below 31.25 MHz, the number of tap weight multiplications available will stay at 4096).

Five different filters were simulated for this memo to show a range of designs that could be programmed in a FIR filter card for the MMA:

FILTER F1	FILTER TYPE	LOWPASS (1/2 band)
	-3 dB POINT	950 MHz
	-40 dB POINT	1000 MHz
	PASS BAND RIPPLE	0.35 dB
	# TAPS	128

FILTER F3	FILTER TYPE	LOWPASS (1/8 band)
	-3 dB POINT	220 MHz
	-46 dB POINT	250 MHz
	PASS BAND RIPPLE	0.20 dB
	# TAPS	256

FILTER F4	FILTER TYPE	LOWPASS (1/2 band)
	-3 dB POINT	900 MHz
	-46 dB POINT	1000 MHz
	PASS BAND RIPPLE	0.06 dB
	# TAPS	128
FILTER F5	FILTER TYPE	LOWPASS (1/64 band)
	-3 dB POINT	25 MHz
	-40 dB POINT	31.25 MHz
	PASS BAND RIPPLE	0.36 dB
	# TAPS	1024
FILTER F7	FILTER TYPE	BANDPASS (1/64 band)
	-3 dB POINTS	1221.5 MHz AND 1246.5 MHz (25 MHz WIDE)
	-40 dB POINTS	1218.375 MHz AND 1249.625 MHz (31.25 MHz WIDE)
	# TAPS	1024

Note that filter F1 and filter F4 are both 1/2 band filters. F1 has a sharper cutoff at the cost of more passband ripple than F4. Whereas filter F1 has 950/1000 or 95% band utilization, F4 has only 90% band utilization.

Figures 2 through 6 show the expected (theoretical) frequency responses for the 5 filters simulated. (The horizontal axis of these plots indicates a frequency range from 0 to 2 MHz. For the MMA application, this can be considered to be from 0 to 2 GHz, being the output of a 4-GHz sampler with an analog 2-GHz width filter in front.)

4. Simulated Input Signal

Three types of input signals were used in the simulations. Figure 7 shows a simulated input signal with a flat spectrum (for MMA purposes, this signal can be considered to be flat from 0 to 2 GHz).

Figure 8 shows the continuum of Figure 7 with four strong spectral lines in the stop band of all filters simulated. The four lines were placed to fall at points 140, 179, 217, and 244 on the 256-point horizontal axis.

The third input drive used to test the filters is seen in Figure 9 which shows the continuum of Figure 7 with a single very strong line falling at horizontal axis point 140.

The lines in Figure 8 are about 22 dB above the noise (considering the bandwidth of the individual points with the 512-point FFT used in the analysis) and the single line in Figure 9 is about 33 dB above the noise floor.

The reason for using the single very strong line in the simulations has to do with a fundamental difference between digital and analog filters: in the digital case, the input sampler will, because of its coarse amplitude quantization, create harmonics of components in the stop band that alias into the passband. Being in the passband, these aliased signals would not be attenuated at all by the digital filter and, hence, the effect should be considered carefully.

5. Simulation Results

In the simulation results given in Figures 10 through 16, the number of samples used is shown at the top of each plot. For example, in Figure 10A, the number of samples is given as $5.937e+007$, so this plot is the result of an integration involving 59.37 million samples (or from a 14.8 millisecond integration considering the 4 GHz sample rate of the MMA).

Figures 10A, 10B, 10C, and 10D show the results of simulating filter F1. Figure 10A shows the frequency response obtained with a flat continuum input signal and a 4-level input sampler. The stop band is down only about 25 dB instead of the 40 dB filter spec. due to the incorrect quantization correction (see Section 2).

Figure 10B shows the response of filter F1 with four strong spectral lines in the stop band. The presence of the spectral lines appears to make the input to the output sampler closer to Gaussian and, hence, the quantization correction yields a stop band floor of about -35 dB. Note the distortion in the passband ripple due to the harmonics of the four lines that alias into the passband (see the discussion of Figure 11A, below).

Figures 10C and 10D duplicate Figures 10A and 10B but with an 8-level sampler driving the simulated filter. Note the absence of distortion in the passband ripple (seen in Figure 10B) in Figure 10D.

Figures 11A and 11B emphasize the difference between using a 4-level input sampler and having an 8-level input sampler. In Figure 11A, the 33 dB strong spectral line at point 140 can be seen attenuated in the filter output by about 58 dB (down to about -25 dB). The third harmonic of the spectral line, aliased to point 92, can be seen in the passband, as can the seventh harmonic aliased to point 44. The ninth harmonic is seen in the stop band aliased to point 236. In Figure 11B, the fundamental is seen attenuated down about 58 dB but no harmonics can be seen at all because the 8-level sampler's odd harmonic generation is less than that for the 4-level sampler.

The other four filters go through the same sequence of four simulations using a 4-level or 8-level sampler at the filter input and having flat or flat with four strong spectral line input signals. (Note that some figures have a 0 to -80 dB vertical scale.)

Figures 12A, 12B, 12C, and 12D show the simulations for the 1/8 band filter F3 (with a 250 MHz MMA bandwidth). Note the slight distortion in the passband of Figure 12B due to harmonics of the spectral lines aliased into the passband. In these figures, the increase in the number of tap weight multiplications (to 256) must make the input signal to the output sampler closer to having a Gaussian distribution because the stop band floor is down to about -40 dB.

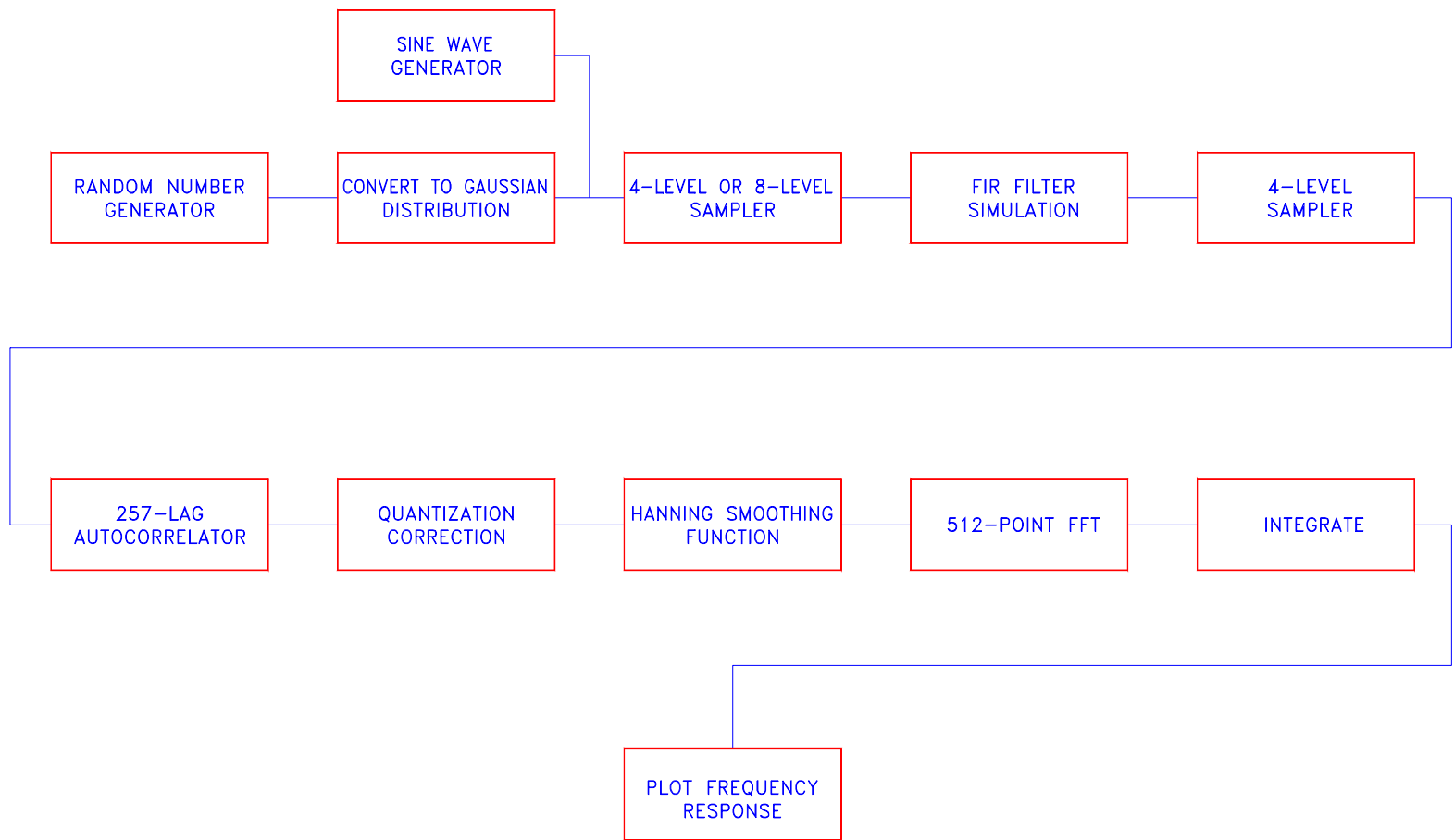
Figures 13A, 13B, 13C, and 13D are for filter F4. Again, note the distortion in the passband of Figure 13B. Figures 14A and 14B show simulation results for Filter 4 using an input signal that includes a single very strong line. In Figure 14A, the third, seventh, and ninth harmonics of the spectral line can be seen but are not visible in Figure 14B.

Figures 15A, 16B, 15C, and 15D give the simulation results for the 31.25 MHz low pass filter F5. Figures 16A through 16D give simulation results for a 31.25 MHz wideband pass filter.

It might be pointed out here that the two $1/64$ band filters, F5 and F7, were each 1024 tap filters. In the system, if a filter is used that has 128 taps available when used in a $1/2$ band configuration, a filter of 32 times 128 or 4096 taps could be implemented (providing higher performance than shown in this memo).

6. Conclusions

The computer simulations presented in this memo seem to indicate that acceptable performance can be obtained if a digital filter is used in the MMA instead of analog filters. The simulations also indicate that the use of an input sampler with greater than 4-level amplitude quantization is desirable (an 8-level sampler would also reduce the loss in sensitivity incurred with the use of two sampler stages).



6

Fig. 1. Flow diagram of simulation software.

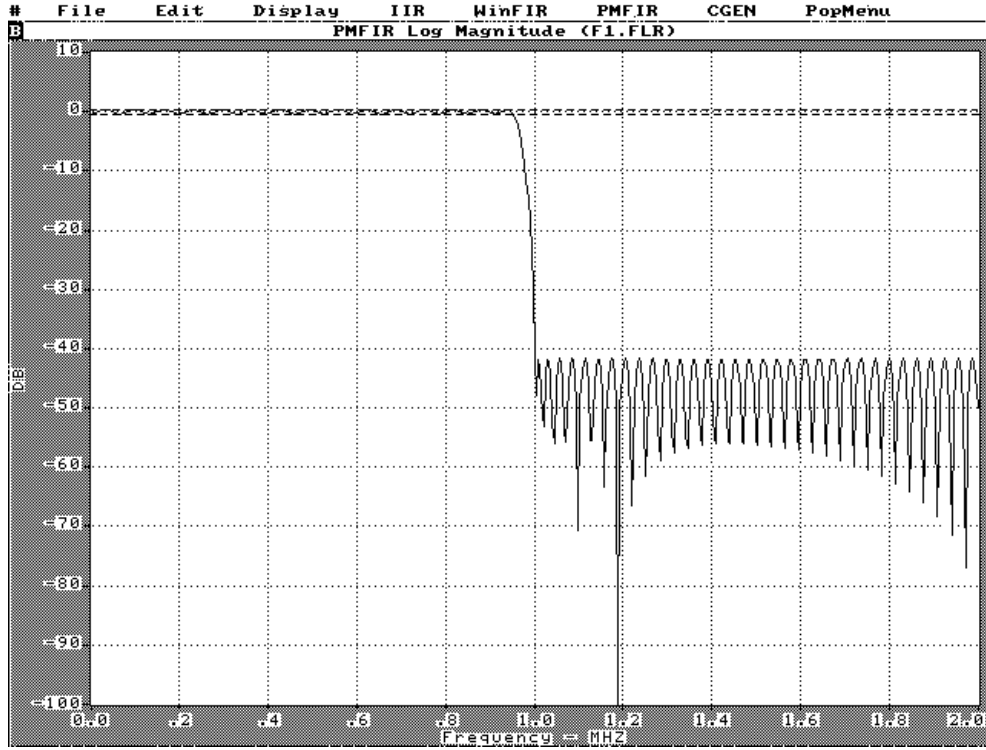


Fig. 2. Filter F1.

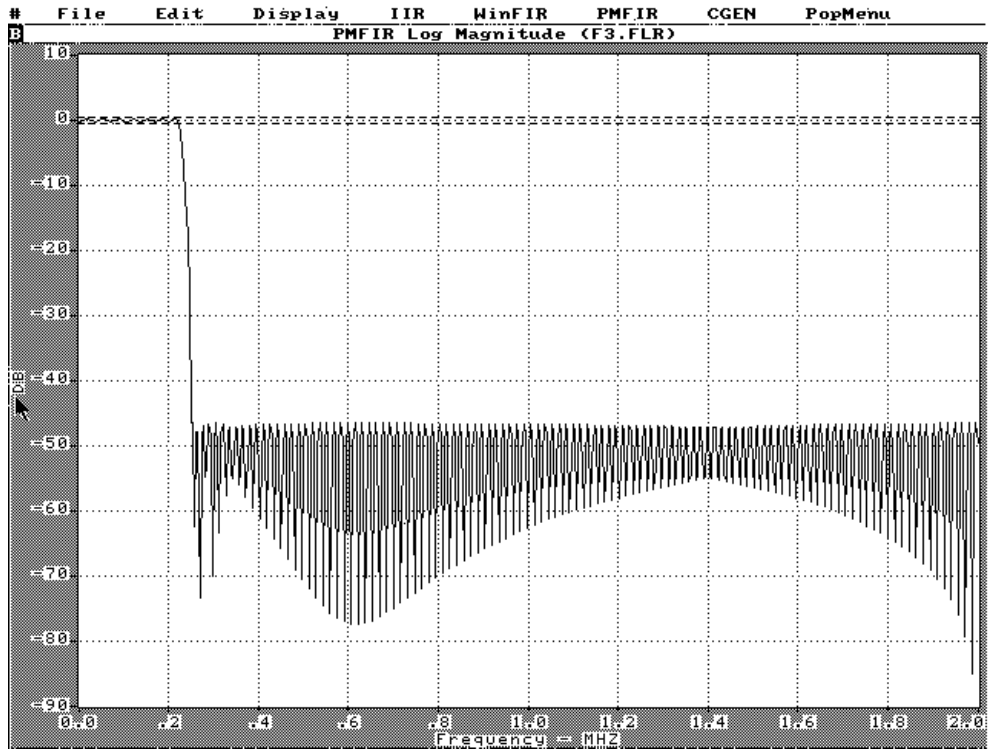


Fig. 3. Filter F3.

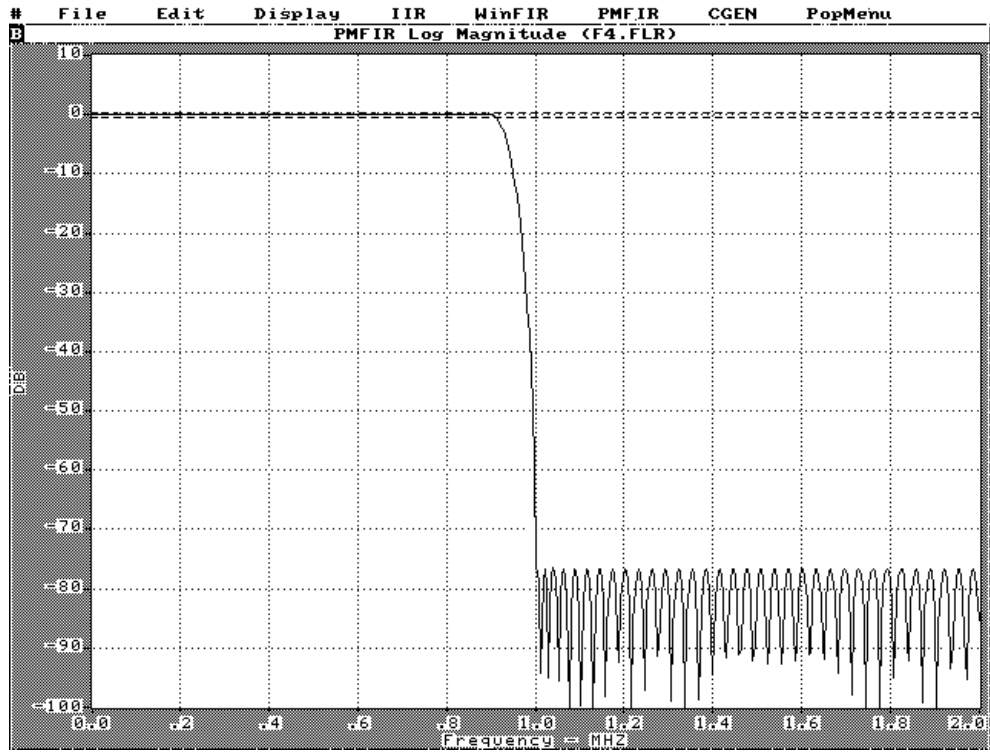


Fig. 4. Filter F4.

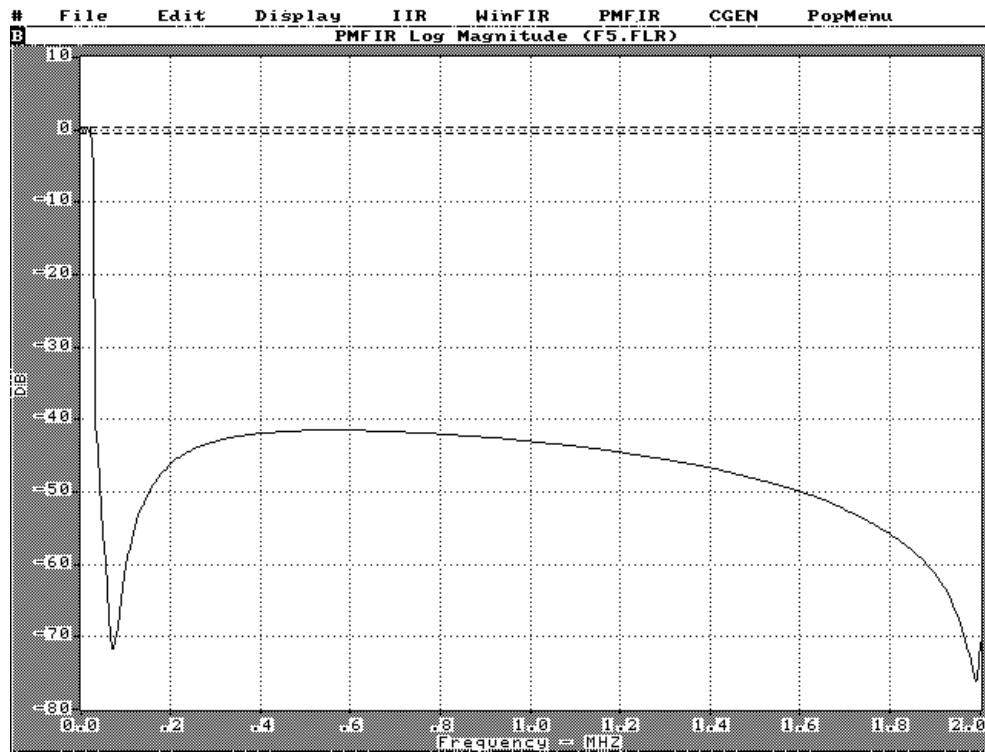


Fig. 5. Filter F5.

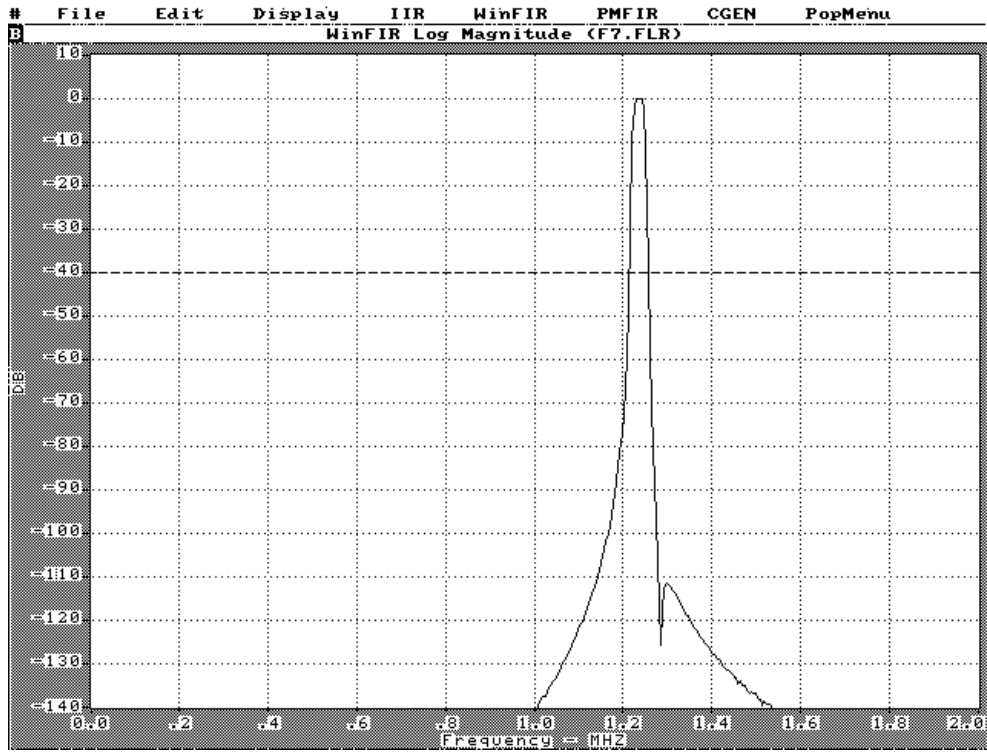


Fig. 6. Filter F7.

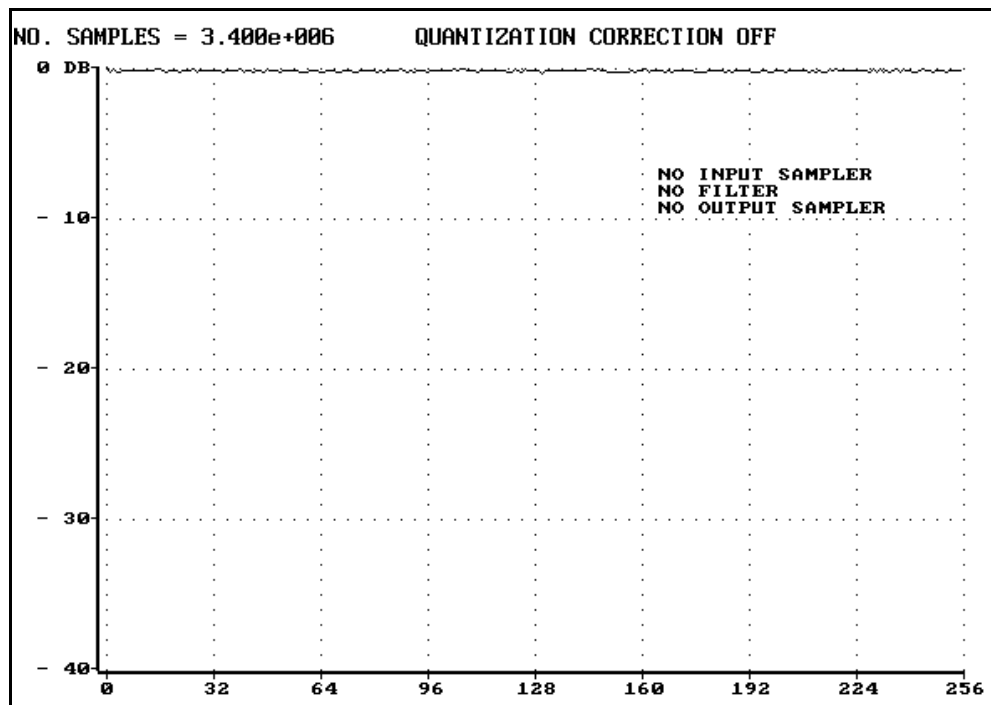


Fig. 7. Continuum input spectrum.

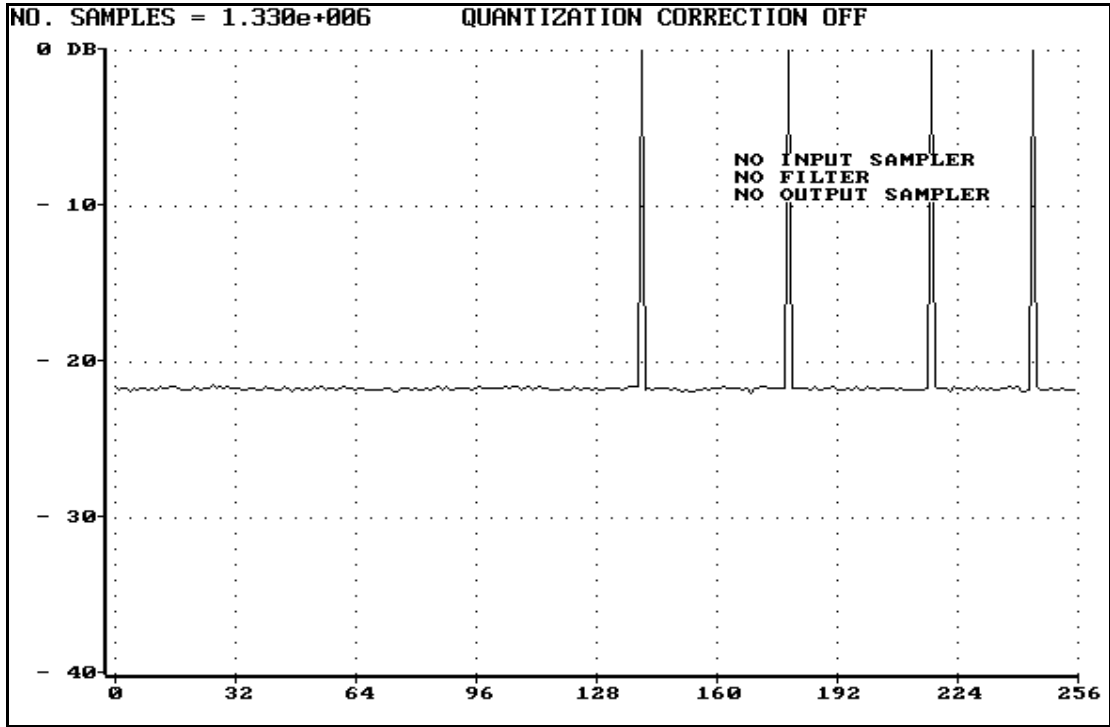


Fig. 8. Continuum with four strong lines

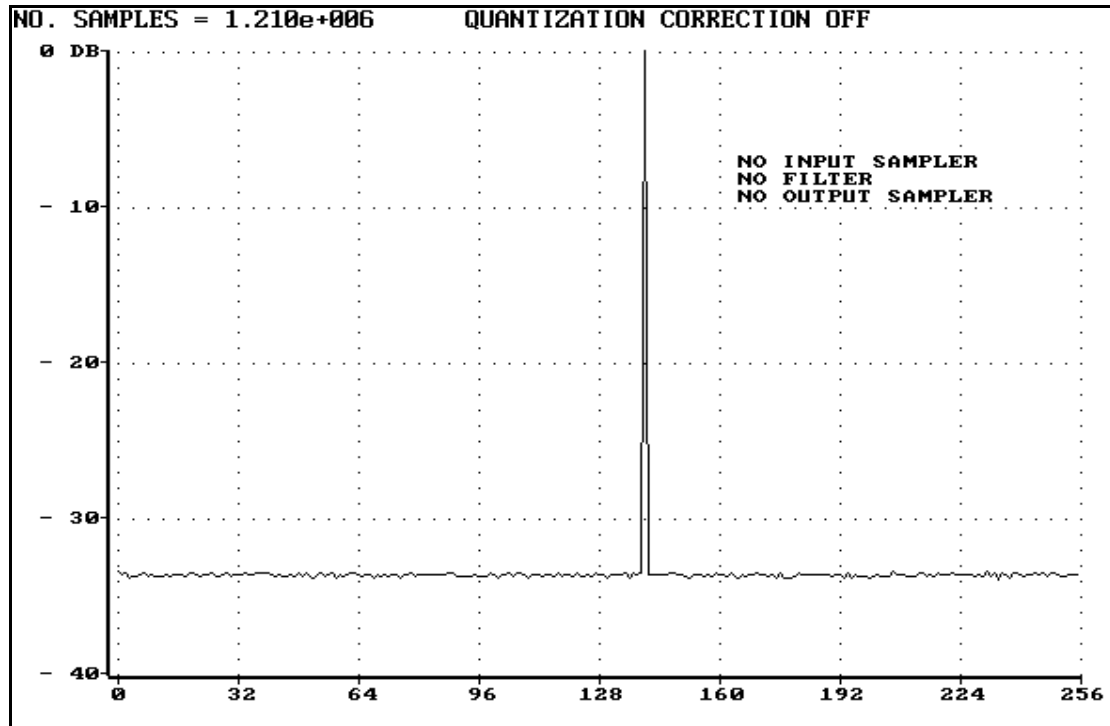


Fig. 9. Continuum with one very strong line.

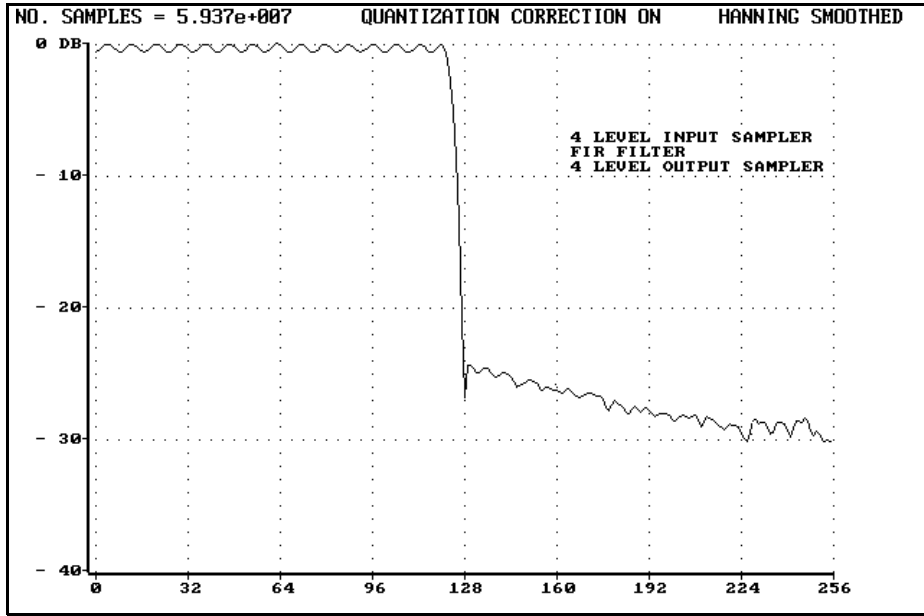


Fig. 10A. Filter F1 frequency response with four-level input sampler and continuum driving signal.

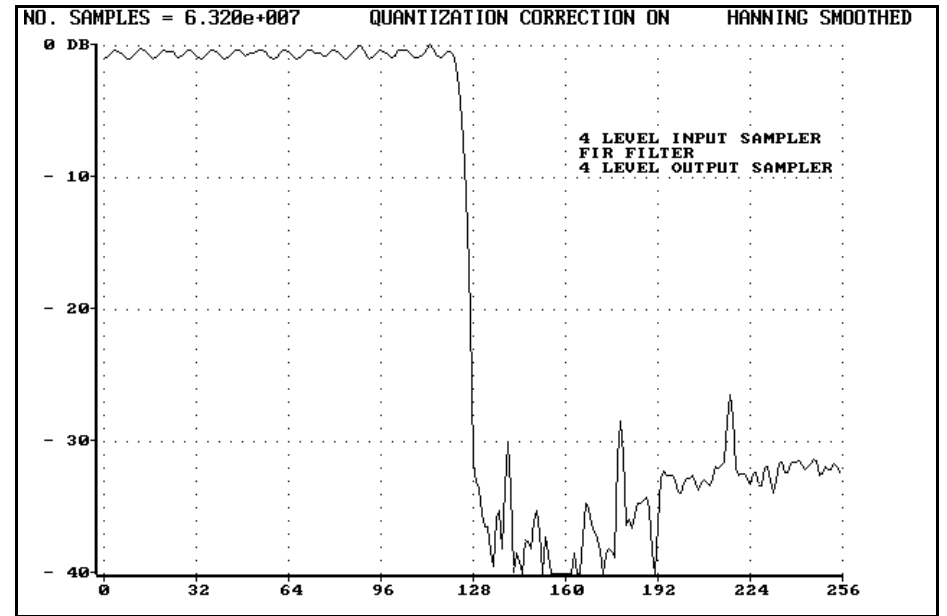


Fig. 10B. Filter F1 frequency response with four-level input sampler and continuum driving signal with four strong lines.

11

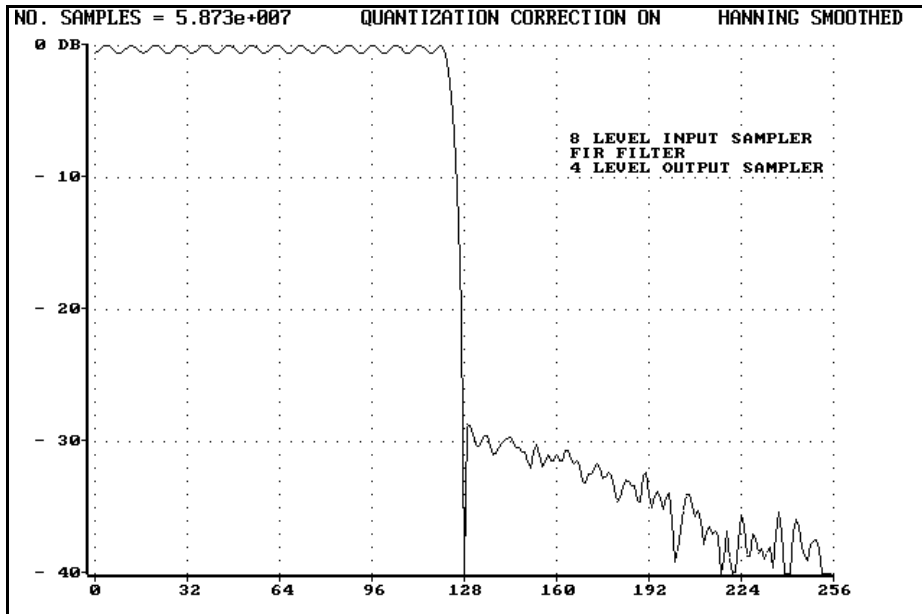


Fig. 10C. Filter F1 frequency response with eight-level input sampler and continuum driving signal.

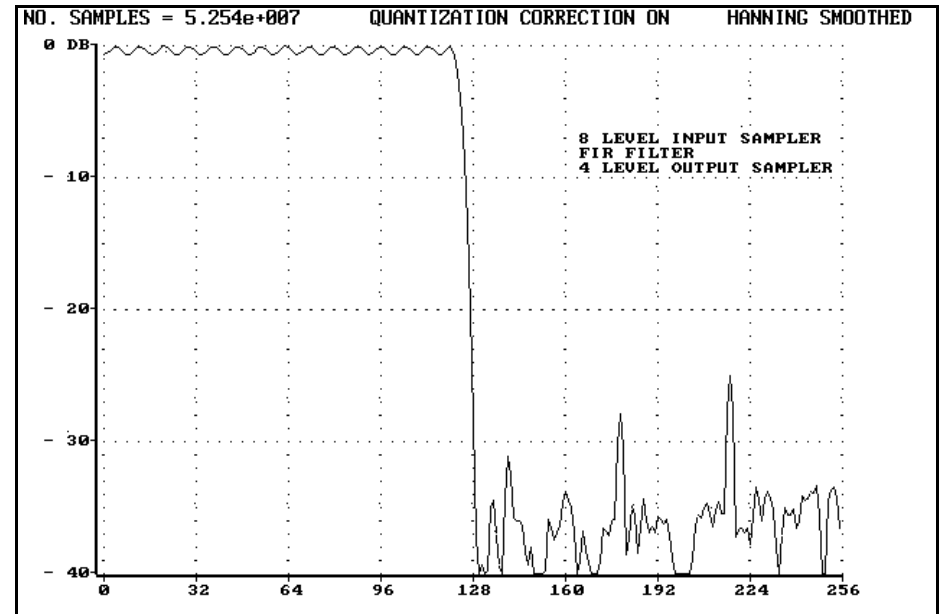


Fig. 10D. Filter F1 frequency response with eight-level input sampler and continuum driving signal with four strong lines.

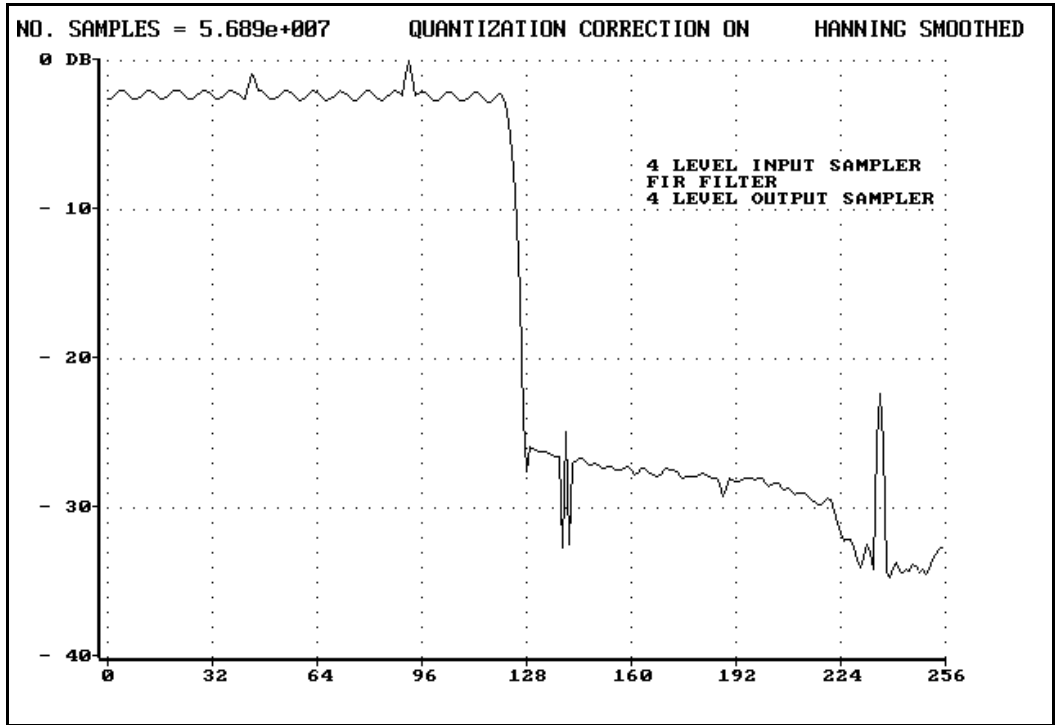


Fig. 11A. Filter 1 frequency response with four-level input sampler and continuum driving signal with one very strong line.

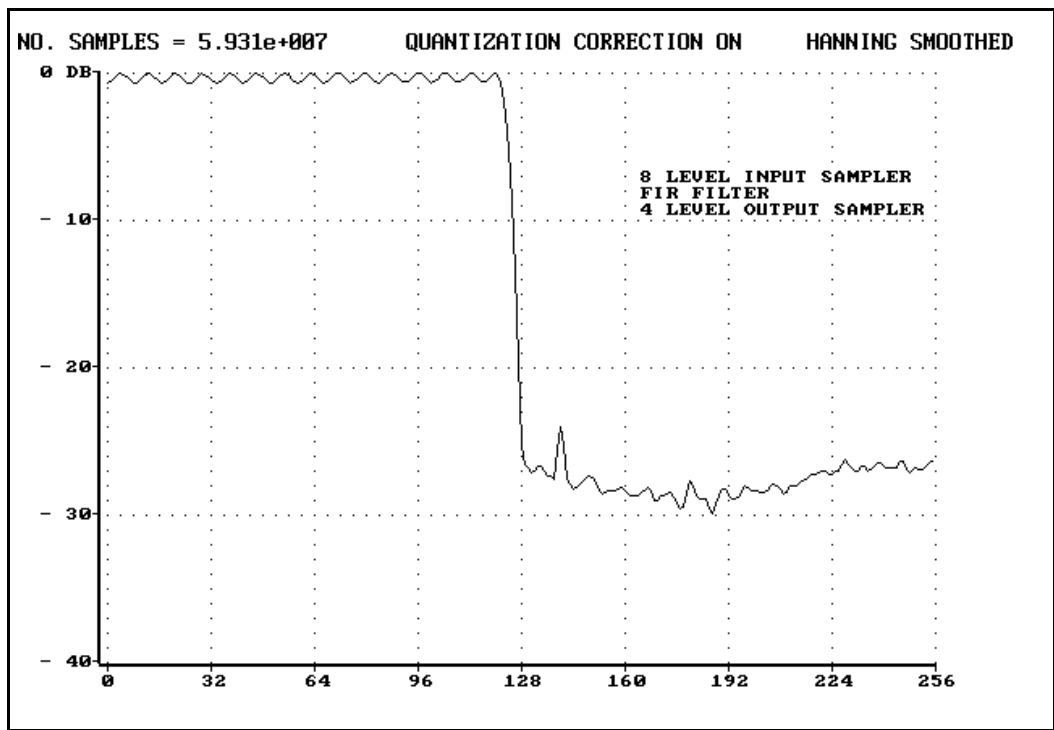


Fig. 11B. Filter 1 frequency response with eight-level input sampler and continuum driving signal with one very strong line.

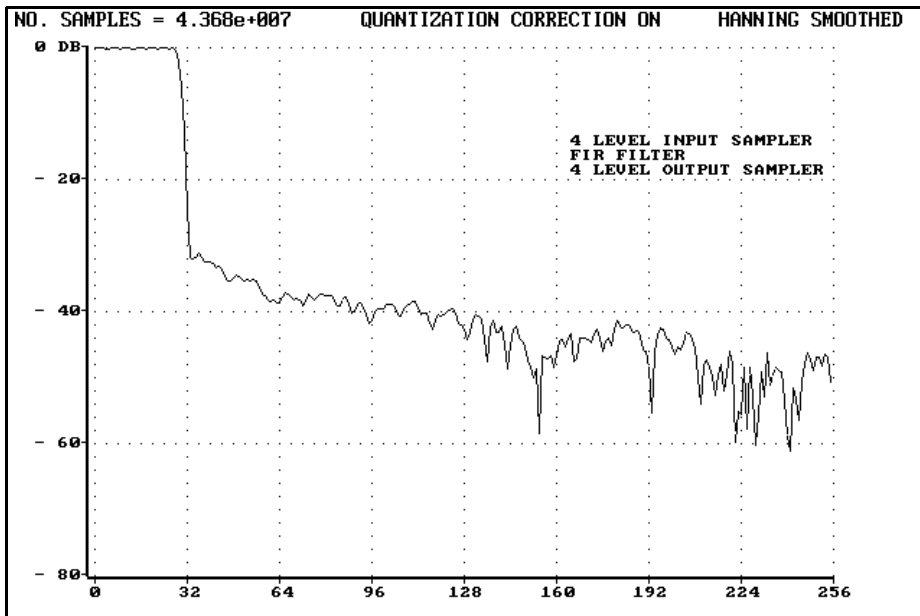


Fig. 12A. Filter F3 frequency response with four-level input sampler and continuum driving signal.

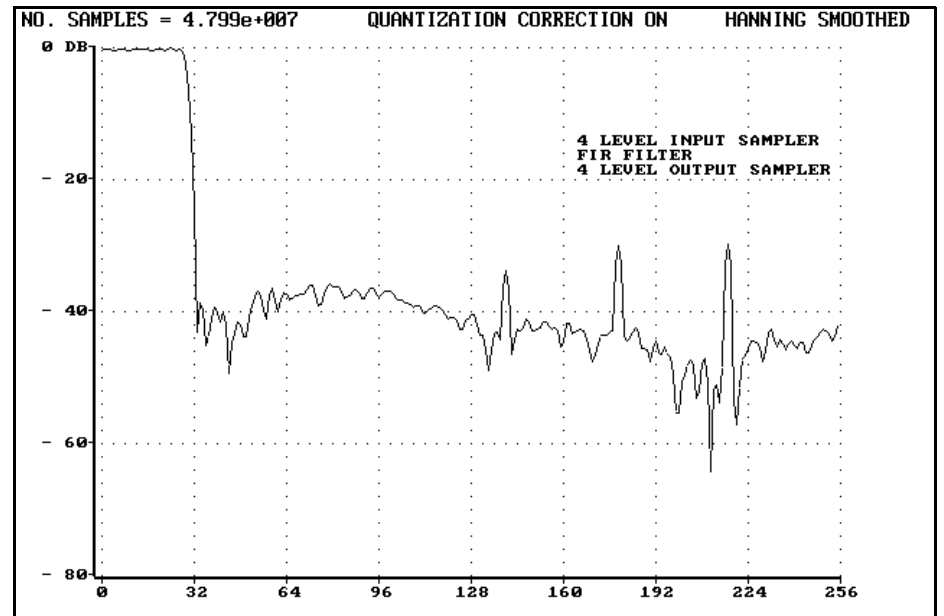


Fig. 12B. Filter F3 frequency response with four-level input sampler and continuum driving signal with four strong lines.

13

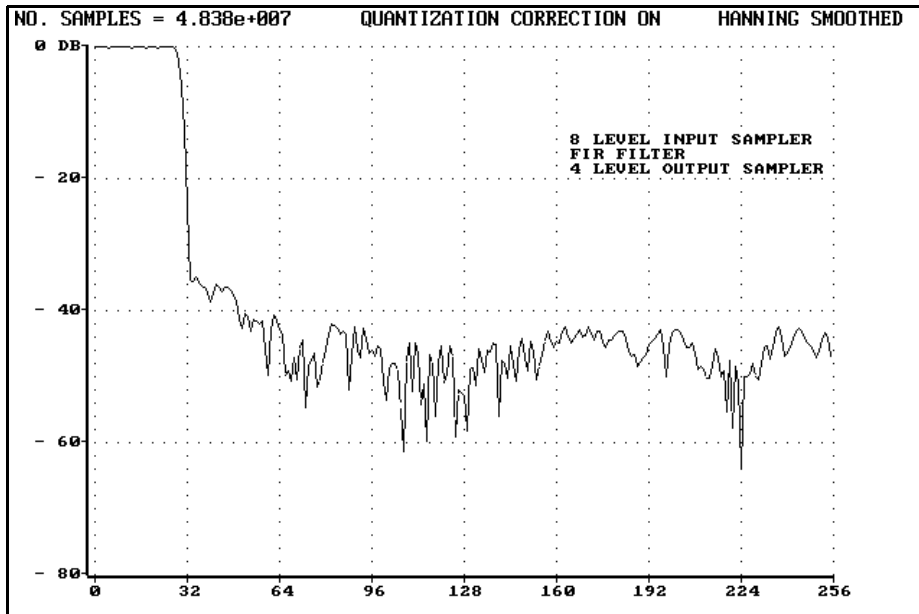


Fig. 12C. Filter F3 frequency response with eight-level input sampler and continuum driving signal.

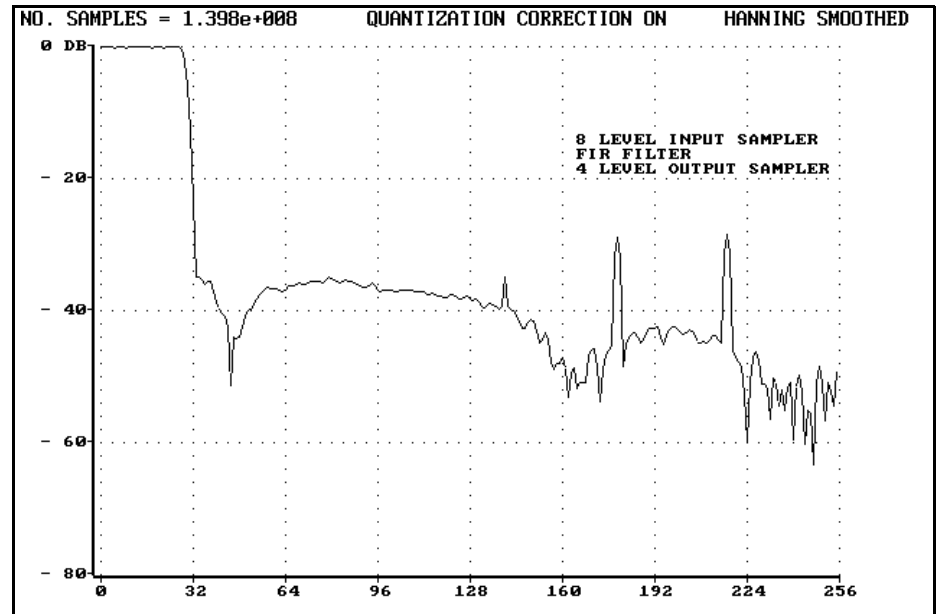


Fig. 12D. Filter F3 frequency response with eight-level input sampler and continuum driving signal with four strong lines.

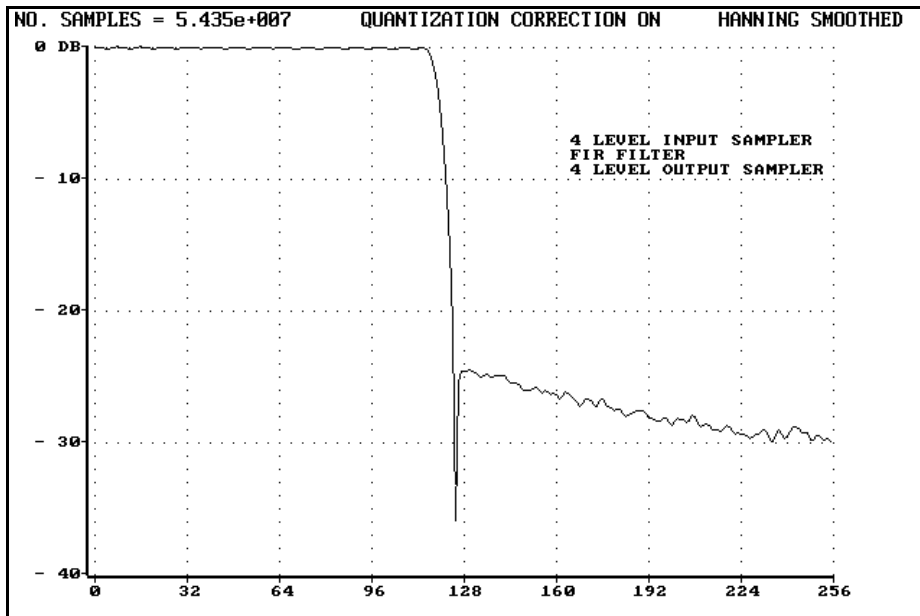


Fig. 13A. Filter F4 frequency response with four-level input sampler and continuum driving signal.

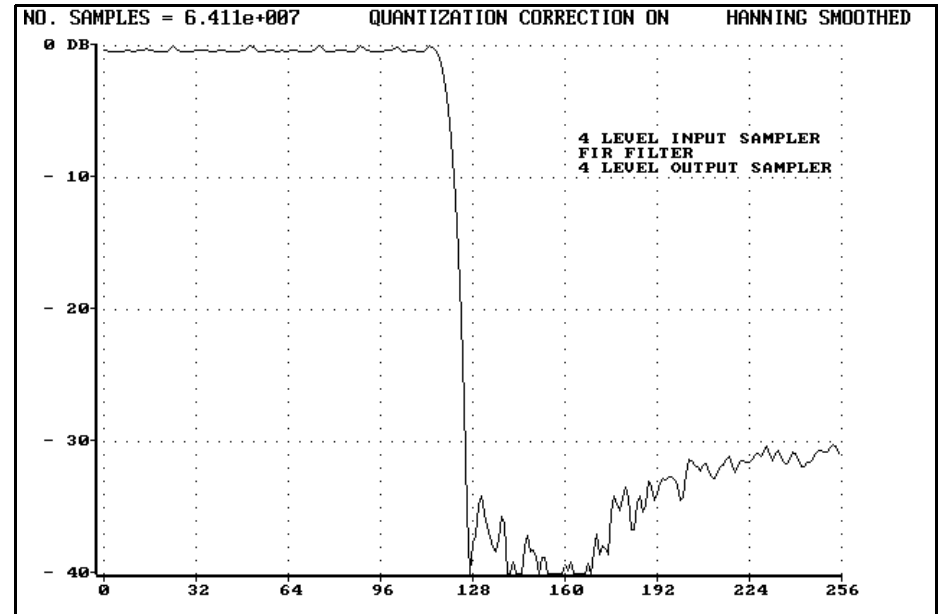


Fig. 13B. Filter F4 frequency response with four-level input sampler and continuum driving signal with four strong lines.

14

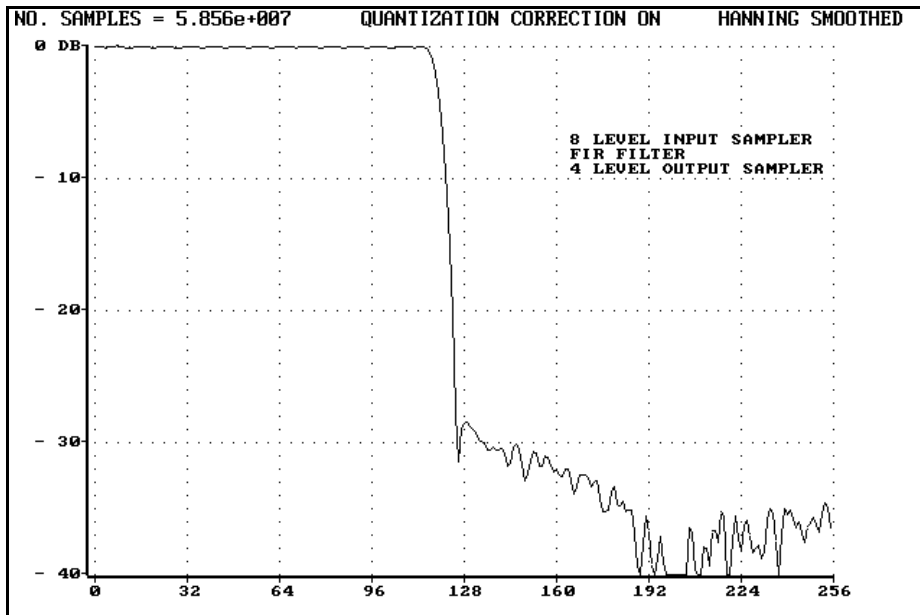


Fig. 13C. Filter F4 frequency response with eight-level input sampler and continuum driving signal.

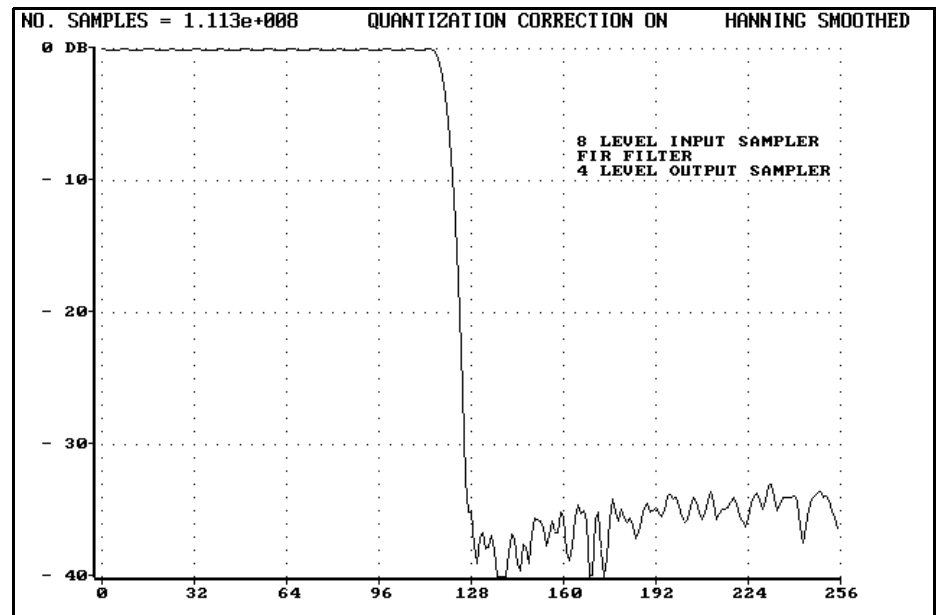


Fig. 13D. Filter F4 frequency response with eight-level input sampler and continuum driving signal with four strong lines.

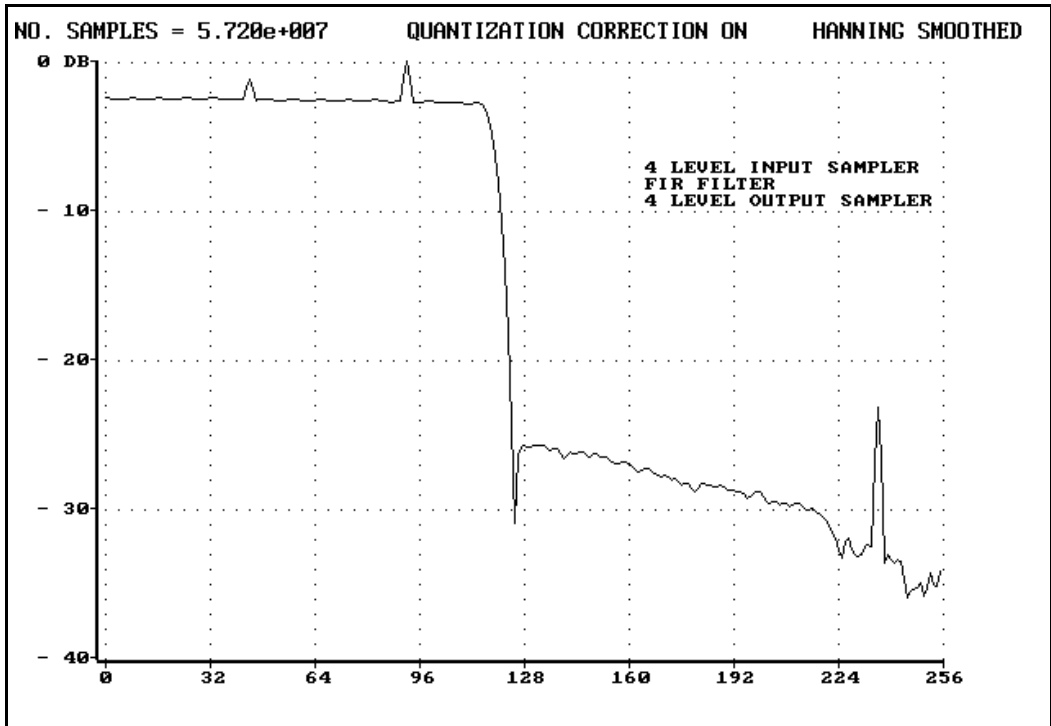


Fig. 14A. Filter 4 frequency response with four-level input sampler and continuum driving signal with one very strong line.

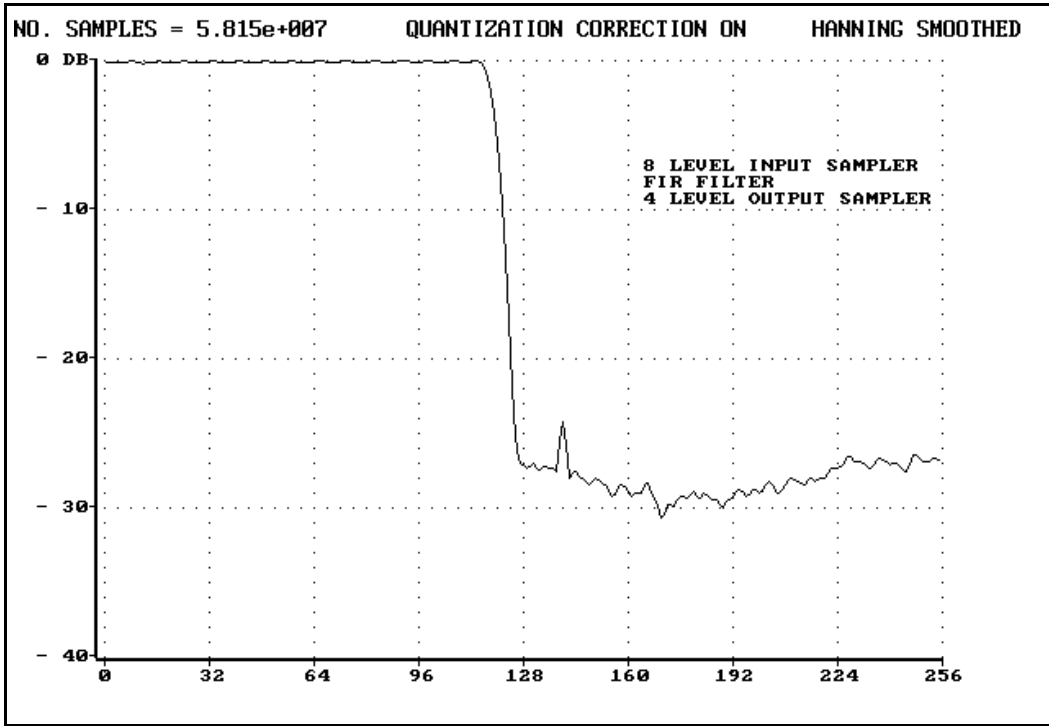


Fig. 14B. Filter 4 frequency response with eight-level input sampler and continuum driving signal with one very strong line.

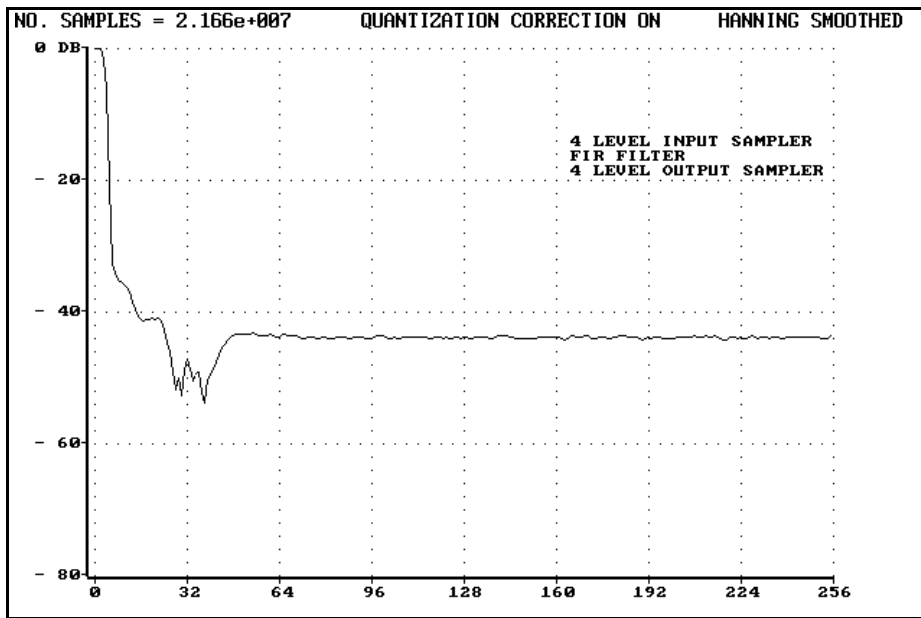


Fig. 15A. Filter F5 frequency response with four-level input sampler and continuum driving signal.

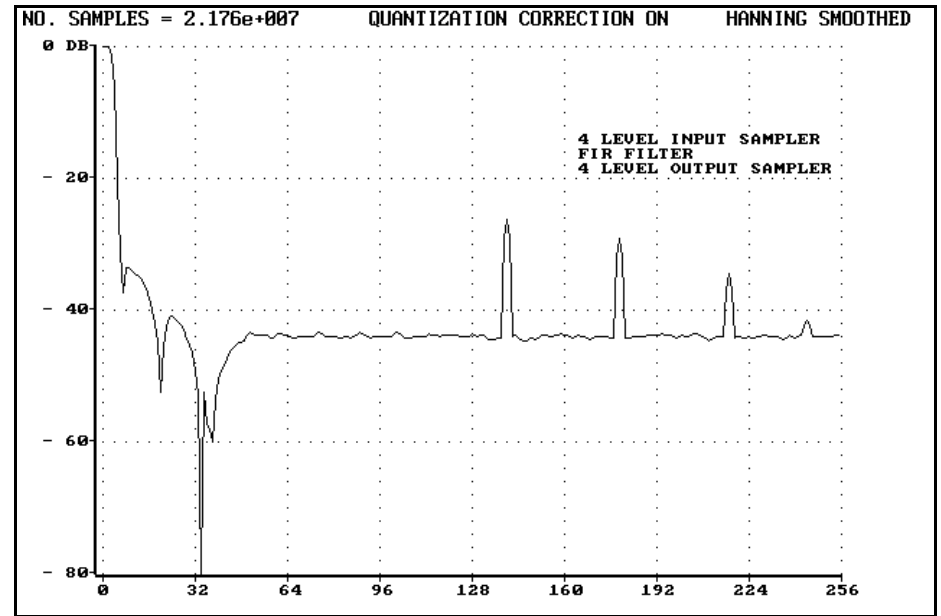


Fig. 15B. Filter F5 frequency response with four-level input sampler and continuum driving signal with four strong lines.

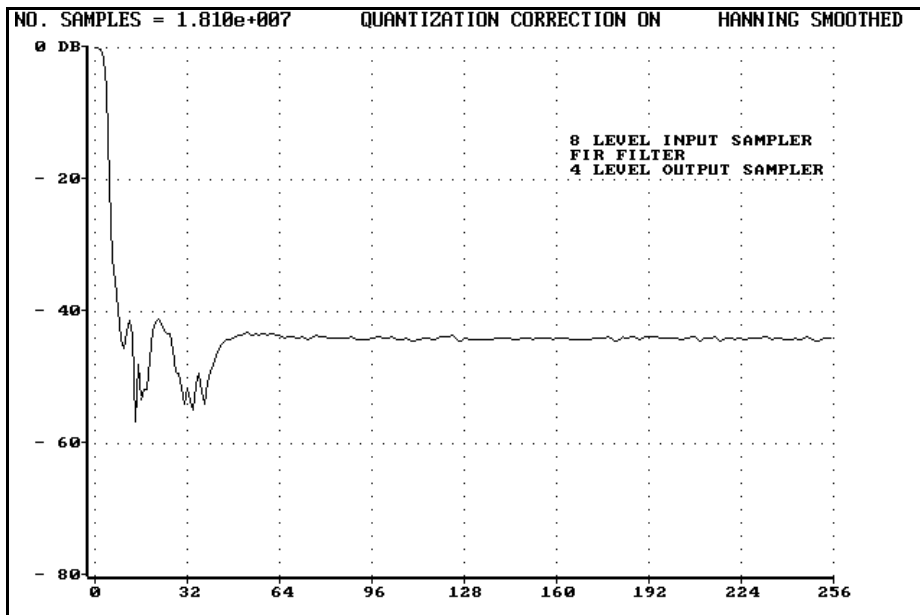


Fig. 15C. Filter F5 frequency response with eight-level input sampler and continuum driving signal.

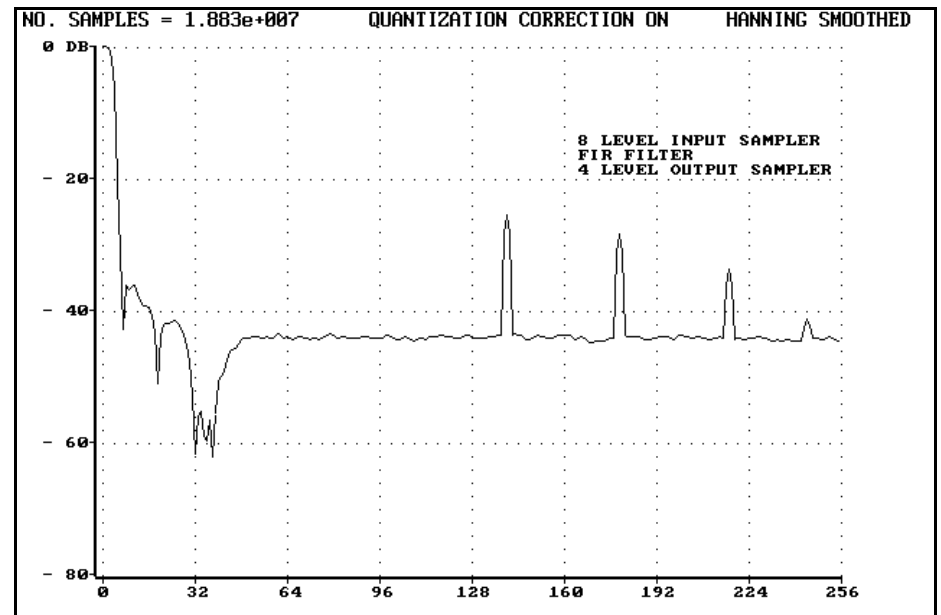


Fig. 15D. Filter F5 frequency response with eight-level input sampler and continuum driving signal with four strong lines.

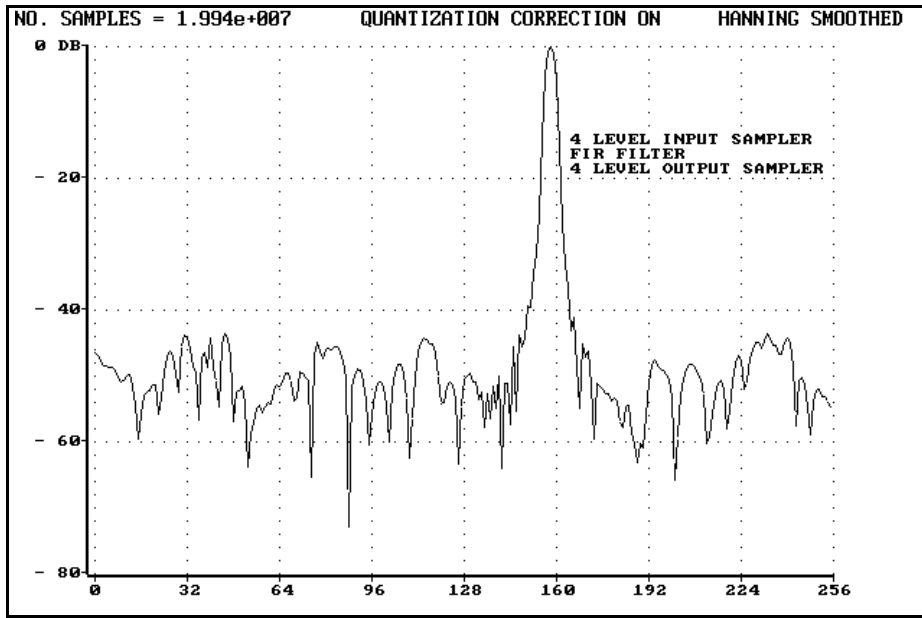


Fig. 16A. Filter F7 frequency response with four-level input sampler and continuum driving signal.

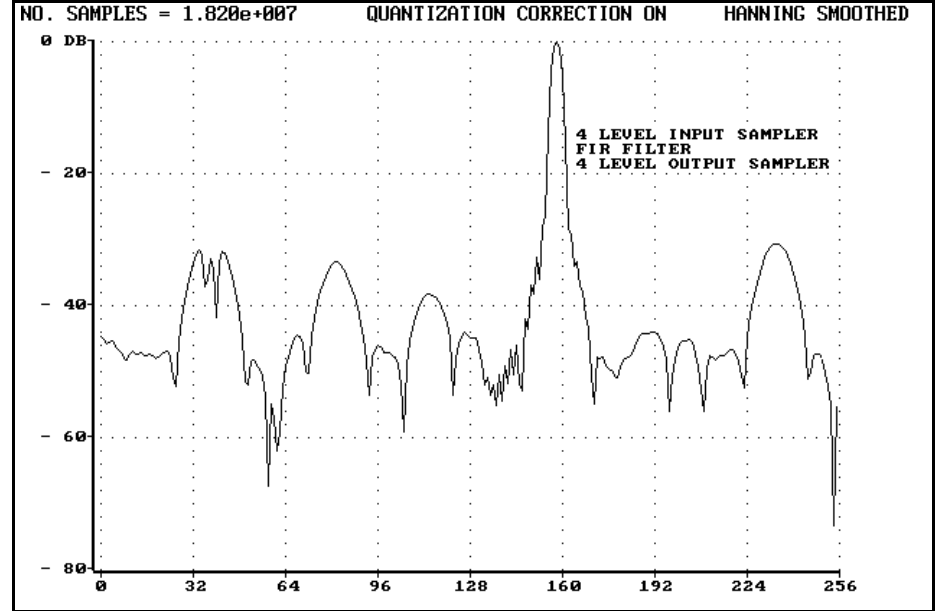


Fig. 16B. Filter F7 frequency response with four-level input sampler and continuum driving signal with four strong lines.

17

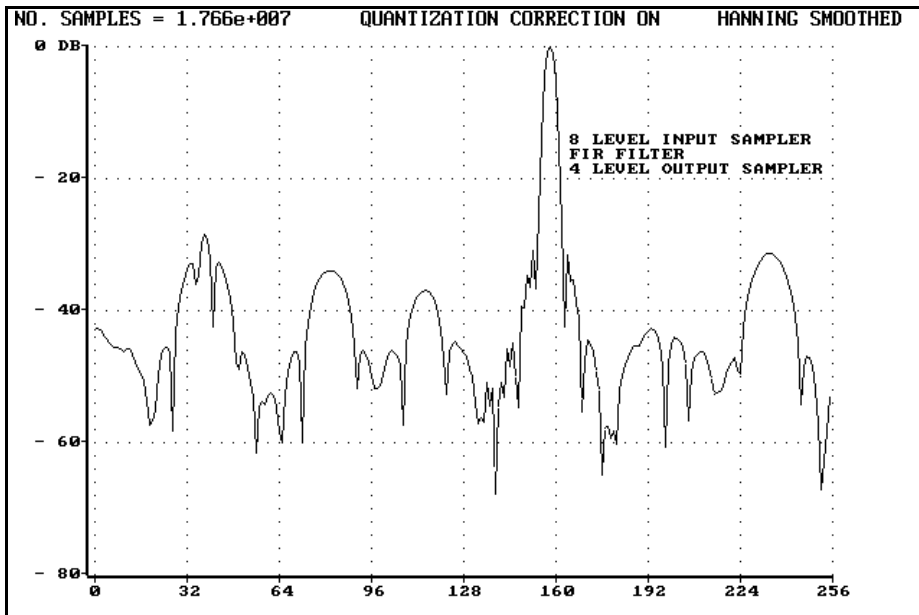


Fig. 16C. Filter F7 frequency response with eight-level input sampler and continuum driving signal.

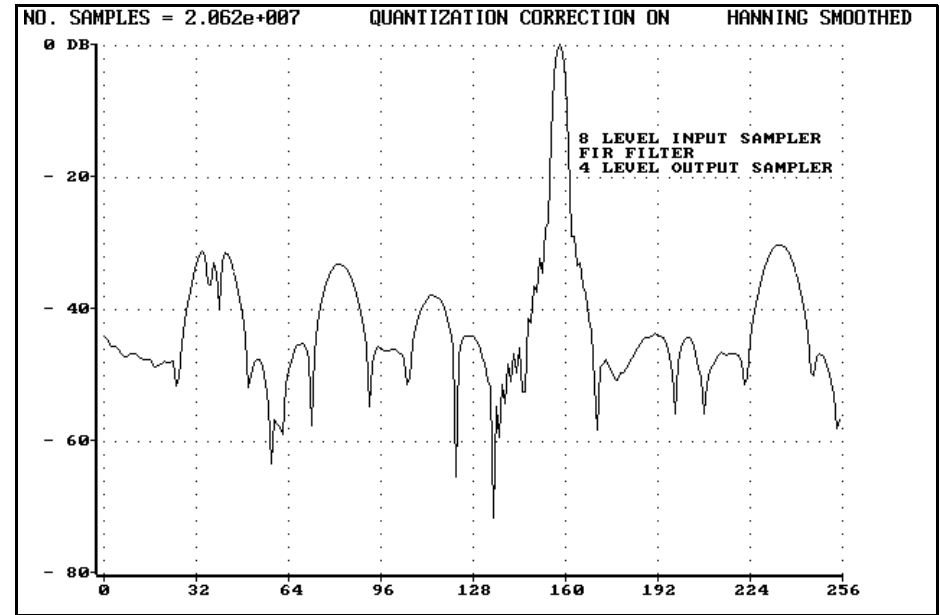


Fig. 16D. Filter F7 frequency response with eight-level input sampler and continuum driving signal with four strong lines.